Determination of the Region of Existence of Ferromagnetic Nanostructures in the Paraphase of $La_{1-x}Ba_xMnO_3$ by the EPR Method

R. M. Eremina[a],*, I. V. Yatsyk[a], Ya. M. Mukovskiĭ[b], H.-A. Krug von Nidda[c], and A. Loidl[c]

[a] *Kazan Physicotechnical Institute, Kazan Scientific Center, Russian Academy of Sciences,*
Sibirskiĭ trakt 10/7, Kazan, 420029 Russia
* e-mail: rushana@kfti.knc.ru

[b] *Moscow State Institute of Steel and Alloys (Technological University), Leninskiĭ pr. 4, Moscow, 119049 Russia*
[c] *Experimentalphysik V, Universität Augsburg, 86135 Augsburg, Germany*

In the paraphase of a number of $La_{1-x}Ba_xMnO_3$ single crystals with $0.1 \leq x \leq 0.2$ below 340 K, signals of the ferromagnetic resonance are observed, which indicates the presence of magnetically ordered nanoscopic objects (ferrons). The region of the existence of ferrons on the Ba density–temperature phase diagram has an approximate triangular shape, which is characteristic of the Griffiths phase. Investigations of the angular and frequency dependences of the position of the ferromagnetic resonance line indicate that the nanostructures have a spherical shape. The parameters of their magnetic anisotropy are found to be $H_{a1} = 2500$ Oe and $H_{a2} = -700$ Oe.

The colossal magnetoresistance is observed in $La_{1-x}Me_xMnO_3$ doped with the bivalent ions Me = Sr, Ba, Ca, etc. The phase diagram of these compounds is very rich [1, 2] and can include regions with phase stratifications [3].

It is known that the magnetoresistance method is highly sensitive. In particular, the electron paramagnetic resonance (EPR) method allows one to confidently detect the presence of magnetic impurities of fractions of a percent. In this work, $La_{1-x}Ba_xMnO_3$ single crystals are studied by the EPR method. The nanoscopic magnetic structures are found near the phase interface of the ferromagnetic–paramagnetic transition on the side of the paraphase. Interest in nanoscopic magnetic objects in manganites has recently increased in view of the colossal magnetoresistance. Hypothetical ferromagnetic nanodomains (ferrons) are important for constructing the theory of the conductance of $La_{1-x}Me_xMnO_3$ manganites, where Me = Sr, Ca, and Ba [4].

The $La_{1-x}Ba_xMnO_3$ single crystals were grown by the crusibleless zone melting method with radiative heating [5]. The measurements of the EPR spectra were performed using Bruker ER 086 CS and Varian E-12 spectrometers equipped with temperature blows for measurements in the temperature range from 4.2 to 600 K at frequencies 9.4 and 34 GHz. The $La_{1-x}Ba_xMnO_3$ single crystals with $x = 0.05, 0.1, 0.12, 0.15, 0.2,$ and 0.3 are studied. The single crystals were

preliminarily oriented using the x-ray diffraction. For EPR study, discs 3 mm in diameter and 0.5 mm in height are cut from the single crystals so that the disc plane is perpendicular to the [110] crystallographic axis for $x = 0.1$ and 0.15 and to the [001] crystallographic axis for $x = 0.12, 0.2,$ and 0.3.

The angular and temperature dependences of the EPR spectra in $La_{1-x}Ba_xMnO_3$ single crystals with $x = 0.05, 0.1, 0.12, 0.15, 0.2,$ and 0.3 are studied in the temperature interval from 200 to 420 K in the X and Q ranges. Several lines are observed in the EPR spectrum for the samples with $x = 0.1, 0.12, 0.15,$ and 0.2 below 340 K to the Curie temperature. The shape of the EPR spectrum for the temperature $T = 290$ K for the $La_{0.8}Ba_{0.2}MnO_3$ single crystal in the X range is shown in the inset in Fig. 1. The most intense line with $g_{eff} \approx 2$ is associated with the narrowed signal from the Mn^{3+} and Mn^{4+} ions and is referred to the paramagnetic region. The features of this signal are not discussed in this paper. Additional lines that are observed in the EPR spectrum and whose intensity at room temperature is six orders of magnitude lower than the line at $g_{eff} \approx 2$ are of primary interest. We emphasize that these additional lines are observed in the EPR spectrum of $La_{1-x}Ba_xMnO_3$ single crystals with $x = 0.1, 0.12, 0.15,$ and 0.2 for temperatures from about 340 K to the phase transition temperature. The effective g factors of signals at room temperature in low and high magnetic fields are estimated from the relation $h\nu = g_{eff}\beta H_{res}$ as 3.71 and
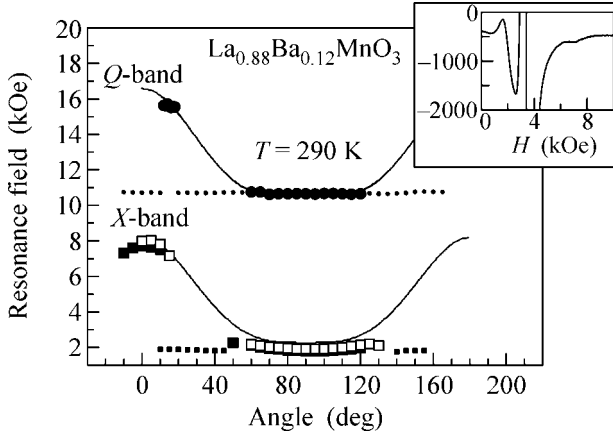
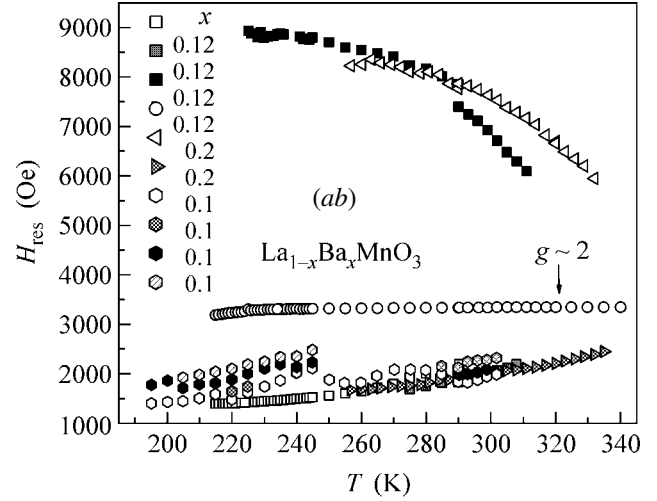**Fig. 1.** Angular dependence of the positions of the additional ferromagnetic lines in the EPR spectrum of the $La_{1-x}Ba_xMnO_3$ single crystal that are detected in the (squares) X and (circles) Q ranges. The solid line is calculated by Eq. (1) with the magnetic anisotropy field $H_{a1} = 2500$ Oe and $H_{a2} = -700$ Oe. The weak additional lines are shown by smaller symbols. The inset shows the spectrum for the $La_{0.8}Ba_{0.2}MnO_3$ single crystal in the X range in the (ab) plane. The ordinate axis shows the relative intensity.

Fig. 2. Temperature dependence of the positions of the additional lines in the EPR spectrum of the $La_{1-x}Ba_xMnO_3$ single crystals in the X range for $x =$ (hexagons) 0.1, (squares) 0.12, and (triangles) 0.2. The circles are the temperature dependence of the paramagnetic signal for $g_{eff} \approx 2$ in the sample with $x = 0.12$.

0.87 in the X range, respectively, and 2.29 and 1.56 in the Q range, respectively. The magnetic anisotropy of the line position in the X and Q ranges does not change and is equal to about 6000 Oe. The above-listed features of the position of additional lines are typical for ferromagnetic resonance [6]. The angular dependences of the position of additional lines in the X and Q ranges are shown in Fig. 1. The points are experimental data and the solid lines are the theoretical calculations of the position of the ferromagnetic resonance line for the spherical sample with tetragonal anisotropy and with the easy magnetization axis. The experimental data are approximated by Eq. (2.2.9) from [6]

$$(\omega/\gamma)^2 = [H_{0z} + 2H_{a1}\cos^2\theta_0 + H_{a2}\sin^2 2\theta_0] \\ \times [H_{0z} + 2H_{a1}\cos 2\theta_0 + 4H_{a2}\sin^2\theta_0(1 + 2\cos 2\theta_0)], \quad (1)$$

where ω is the microwave frequency, γ is the gyromagnetic ratio, and H_{a1} and H_{a2} are the magnetic anisotropy parameters. To determine the form of ferrons, the angular dependence of the EPR spectra is measured out of the disc plane. Ferromagnetic resonance lines are also observed in the EPR spectrum above the Curie temperature T_c. Their angular dependence is almost the same as the angular dependence of the ferromagnetic resonance line detected in the disc plane, which confirms the hypothesis of the spherical shape of ferromagnetic domains. For $La_{1-x}Ba_xMnO_3$ samples with a barium content of 5 and 30%, no additional signal of the ferromagnetic resonance is observed in the EPR spectrum of the paramagnetic phase.

Figure 2 shows the temperature dependence of the positions of the lines in the X range of the EPR spectrum. The resonance signal field with $g_{eff} \approx 2$ remains almost unchanged in the paraphase. The ferromagnetic resonance lines in $La_{1-x}Ba_xMnO_3$ for $x = 0.1$, 0.12, 0.15, and 0.2 are pronounced at temperatures below 310 K. When temperature increases, they are shifted towards the line with $g_{eff} \approx 2$. In the temperature range 310–340 K, the separation of these signals is almost impossible, because the intensity of the ferromagnetic resonance lines is six orders of magnitude smaller than the line for a g factor of 2, and the lines of paramagnetic and ferromagnetic resonances are imposed on each other. It is worth noting that the ferromagnetic resonance line is split into several components close to the field in dependence on the temperature in the paraphase. In particular, the lines near $g_{eff} \approx 4.69$ at $T = 215$ K are sufficiently narrow, and the width of the last low-field line is equal to 60 Oe. This property is obviously associated with a certain spread of the magnetic anisotropy parameters in the ferromagnetic domains. For a temperature of 275 K, all these lines are joined in one line with a width of about 500 Oe, and the amplitude of the total signal is approximately 540 times smaller than the amplitude of the main signal for $g \approx 2$. The observation of the spectral lines that have the intensity an order of magnitude smaller than the main ferromagnetic resonance signal and are shifted from this signal by 90° is associated with the twinning of $La_{1-x}Ba_xMnO_3$ single crystals.

Summarizing all these features, one can plot the region of coexistence of the paramagnetic and ferro-

magnetic regions on the (barium density–temperature) phase diagram. Figure 3 shows the phase diagram of $La_{1-x}Ba_xMnO_3$ single crystals, where the temperatures of the magnetic phase transition are taken from the literature (see the caption of Fig. 3). The asterisks denote the temperatures below which the ferromagnetic resonance lines are observed in the EPR spectrum for the barium ion density from 0.1 to 0.2. The temperature at which an additional ferromagnetic signal appears in the EPR spectrum is almost independent of the barium ion density in the doping range $x = 0.1$–0.2 and is equal to about 340 K. It is seen that the region of the existence of ferrons in the paramagnetic phase has the triangular shape, which is characteristic of the Griffiths phase [7]. Another feature of the Griffiths phase, the temperature behavior of the magnetic susceptibility, is not described by the Curie–Weiss law, but is described by the power function $\chi \sim 1/T^\alpha$, where $\alpha \approx 0.9$. Such a feature of the Griffiths phase was observed in [8] for cobalt-ion doped $CuGeO_3$. A similar behavior is observed in our case, where the integral intensity of the EPR signal, which is proportional to the magnetic susceptibility, in the $La_{0.9}Ba_{0.1}MnO_3$ single crystal for $g_{eff} \approx 2$ from 200 to 340 K is not described by the Curie–Weiss law. The behavior of the magnetic susceptibility in $La_{0.7}Ca_{0.3}MnO_3$ was considered in the Griffiths model in [9].

The region of the existence of the Griffiths phase that we determine is similar to that found in [10] for $La_{1-x}Sr_xMnO_3$ at temperatures below 270 K and strontium density from 7.5 to 17.5%, but it is shifted towards higher temperatures by about 70 K. The feature indicated above is of interest for the synthesis of new materials with the Griffiths phase in a desired temperature range. The Griffiths theory was developed for diluted Ising ferromagnetic materials. As shown in [7], nuclei of the ferromagnetic phase are formed in the paramagnetic phase below the so-called Griffiths temperature T_G to the phase transition temperature T_c depending on the disorder parameter p. The Ba^{2+} ions are responsible for disorder in the case of manganites. It is assumed that the Ba^{2+} ions substitute for La^{3+} ions and simultaneously a hole distributed over the sites of Mn^{3+} ions or oxygen appear. Migrating between different Mn^{3+} sites, the hole polarizes the spin direction, which leads to the formation of ferromagnetically ordered microdomains. These regions must obviously not be too large. We observe ferrons at $x = 0.2$, i.e., when the barium ions are located in each fifth cell; hence, the diameter of a ferron must be no larger than five lattice periods. The existence of ferromagnetic regions in the paramagnetic state leads to phase stratification in manganites. Using this assumption, Kugel' et al. [4] analyzed the temperature dependence of the magnetoresistance, conductivity, and magnetic susceptibility for various manganite types. The sizes of ferromagnetically correlated regions are six or seven lattice periods, and the magnetic anisotropy is approximately equal to 2000 Oe, which approx-
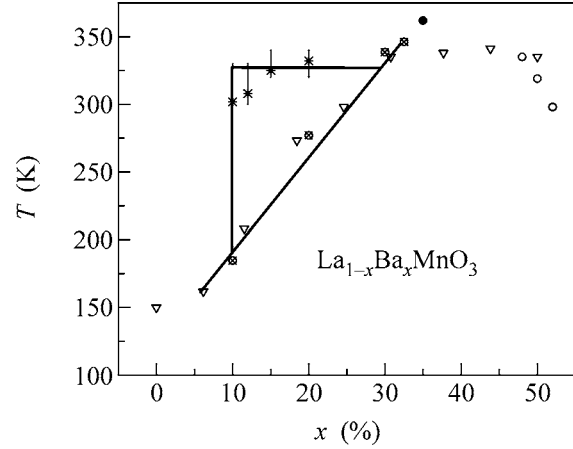
Fig. 3. Phase diagram of $La_{1-x}Ba_xMnO_3$. The asterisks denote the temperatures below which the ferromagnetic resonance lines are observed in the EPR spectrum. The temperatures of the paramagnetic–ferromagnetic phase transition are taken from ($\circ$) [16], ($\bullet$) [17], ($\triangledown$) [2], and ($\otimes$) [1].

imately coincides with our estimates. The estimates of the parameters of ferrons are quite close to each other for manganites with different contents and transport properties.

It is worth noting that the magnetic anisotropy of the position of the ferromagnetic resonance line is almost the same for manganites of all contents and is equal to about 6000 Oe, as in [10] for $La_{1-x}Sr_xMnO_3$ with $0.075 \le x \le 0.175$. In this case, the difference between the positions of the paramagnetic EPR signal and ferromagnetic signal in low fields is equal to 1000 Oe. It is interesting that the lines of both paramagnetic resonance and ferromagnetic resonance are observed in the EPR spectra from $Eu_{0.7}Pb_{0.3}MnO_3$ single crystals for temperatures from 120 to 235 K [11]. The difference between the positions of the ferromagnetic resonance line in low fields and paramagnetic resonance is independent of the microwave frequency at which the experiment is carried out and is equal to about 1000 Oe, as well as for $La_{1-x}Sr_xMnO_3$ and for $La_{1-x}Ba_xMnO_3$ single crystals. The angular dependence of the position of the ferromagnetic resonance line was not studied in [11], because the ferromagnetic resonance line and paramagnetic resonance line were imposed on each other.

Let us briefly discuss an alternative possibility of explaining our data by using the hypothesis that doping with barium ions is strongly inhomogeneous over the sample. In this case, the internal magnetic anisotropy of these regions is expected to coincide with the data on the ferromagnetic resonance below the Curie temperature, but the magnetic anisotropy of low-field and high-field positions of this signal for $La_{0.8}Sr_{0.2}MnO_3$ is equal to about 800 Oe at 50 K [12]. This quantity for ferrons is equal to 6000 Oe. One can assume that the size and internal magnetic anisotropy of ferrons formed in the

paramagnetic region above the phase transition temperature are common features inherent in all manganites.

Ferromagnetically ordered hole-enriched nanodomains in $La_{1-x}Ca_xMnO_3$ manganites are also observed by neutron scattering methods in [13], where it was found that the ferromagnetic regions with a diameter of 20 Å, i.e., about five lattice periods, as in our case, are observed in the ordered antiferromagnetic ground state.

The introduction of divalent Sr or Ba impurities with ion radii of 0.120 and 0.138 nm, respectively, at the site of the La ion (0.104 nm) strongly distorts the crystal lattice and leads to an unordinary temperature behavior of the lattice parameters near the phase transition temperature, as indicated in [14] for $La_{1-x}Ba_xMnO_3$ single crystals. It has been found that the orthorhombic and rhombohedral phases coexist in the single crystal with $x = 0.15$ in a temperature range wider than 150° from 150 to 310 K. Heating above 310 K and cooling below 150 K lead to a single-phase state. The coexistence of two structure phases in the single crystal with $x = 0.20$ [15] was observed from 180 to 200 K.

Thus, using the magnetic resonance method, we found that $La_{1-x}Ba_xMnO_3$ single crystals below the temperature T_G consist of ferromagnetic nanodomains (ferrons) chaotically located in the paramagnetic phase. The data on the ferromagnetic resonance and magnetic susceptibility show that the ferromagnetic regions have the spherical shape with a radius of about 16 Å. The parameters of their magnetic anisotropy are found to be $H_{a1} = 2500$ Oe and $H_{a2} = -700$ Oe. The region of the coexistence of ferrons in the paramagnetic phase on the phase diagram is bounded in the barium concentration from approximately 0.1 to 0.2, $T_G \approx 340$ K, and the phase transition temperature.

REFERENCES

1. J. Zhang, H. Tanaka, T. Kanki, et al., Phys. Rev. B **64**, 184404 (2001).
2. H. L. Ju, Y. S. Nam, J. E. Lee, and H. S. Shin, J. Magn. Magn. Mater. **219**, 1 (2000).
3. É. L. Nagaev, Usp. Fiz. Nauk **166**, 833 (1996) [Phys. Usp. **39**, 781 (1996)].
4. K. I. Kugel', A. L. Rakhmanov, A. O. Sboĭchakov, et al., Zh. Éksp. Teor. Fiz. **125**, 648 (2004) [JETP **98**, 572 (2004)].
5. D. Shulyatev, N. Kozlovskaya, R. Privezentsev, et al., J. Cryst. Growth **291**, 262 (2006).
6. A. G. Gurevich, *Magnetic Resonance in Ferrites and Antiferromagnets* (Nauka, Moscow, 1973), p. 85 [in Russian].
7. R. B. Griffiths, Phys. Rev. Lett. **23**, 17 (1969).
8. S. V. Demishev, A. V. Semeno, N. E. Sluchanko, et al., Fiz. Tverd. Tela (St. Petersburg) **46**, 2164 (2004) [Phys. Solid State **46**, 2238 (2004)].
9. M. B. Salamon, P. Lin, and S. H. Chun, Phys. Rev. Lett. **88**, 197203 (2002).
10. J. Deisenhofer, D. Braak, H.-A. Krug von Nidda, et al., Phys. Rev. Lett. **95**, 257202 (2005).
11. N. Volkov, G. Petrakovskii, K. Sablina, and K. Patrin, Acta Phys. Pol. A **105**, 69 (2004).
12. J. Deisenhofer, H.-A. Krug von Nidda, A. Loidl, et al., Acta Phys. Pol. B **34**, 847 (2003).
13. M. Hennion, F. Moussa, P. Lehouelleur, et al., Phys. Rev. Lett. **94**, 057006 (2005).
14. V. S. Gaviko, N. G. Bebenin, and Ya. M. Mukovskiĭ, in *Abstracts of 9th International Symposium on Ordering in Metals and Alloys* (RGPU, Rostov-on-Don, 2006), p. 103.
15. V. E. Arkhipov, N. N. Bebenin, V. P. Dyakina, et al., Phys. Rev. B **61**, 11229 (2000).
16. O. Chmaissem, B. Dabrowski, S. Kolesnik, et al., Phys. Rev. B **72**, 104426 (2005).
17. R. Vidya, P. Ravindran, P. Vajeeston, et al., Phys. Rev. B **69**, 092405 (2004).

Translated by R. Tyapaev